

The Effects of EDFA Noise on the Performance of Multi-wavelength OCDM-based Long-Reach Passive Optical Networks

Bui Trung Ninh

Department of Netw. and Commun. Systems
Univ. of Engineering and Technology, VNU-Hanoi
Hanoi city, Vietnam
Email: ninhbt@vnu.edu.vn

Ngoc T. Dang

Faculty of Telecommunications
Posts & Telecom. Inst. Tech.
Hanoi city, Vietnam
Email: ngocdt@ptit.edu.vn

Anh T. Pham

Computer Communications Lab.
The University of Aizu
Aizu-Wakamatsu city, Fukushima, Japan
Email: pham@u-aizu.ac.jp

Abstract—In this paper, we propose a model of Long-reach Passive Optical Network (LR-PON) using multi-wavelength optical code-division multiplexing (OCDM) and Erbium-doped fiber amplifier (EDFA). In addition, we analyze the effects of EDFA noise on the performance of OCDM-based LR-PON. Other noise and interference such as shot noise, thermal noise, beat noise, and multiple-access interference (MAI) are included in our theoretical analysis and simulation. We found that the location of EDFA on the link between OLT and ONUs plays an important role in network design since it affects network performance. According to the simulation results, to achieve low bit error rate, the EDFA should be located around 15 to 25 km from OLT when total link distance of 90 km.

I. INTRODUCTION

The explosive demand for bandwidth is leading to the deployment of passive optical networks (PONs), which are able to bring the high-capacity optical fiber closer to the residential homes and small businesses. Long-reach (LR) PON is a recently proposed cost-effective architecture for combining the metro and access networks. This architecture allows the extension of access networks from today's standard of 20 km to 100 km with protection mechanism [1], [2].

A number of LR optical access technologies have been proposed. Initially, the networks were single channel, where a single wavelength is shared between all users, using time division multiplexing (TDM). These networks were followed by wavelength division multiplexing (WDM) ones that shared a number of wavelengths between groups of users. Recently, optical code-division multiplexing (OCDM) has been regarded as a promising candidate thanks to its advantages over conventional techniques, including asynchronous access, efficient use of resource, scalability and inherent security [3].

In OCDM, the signal can be encoded using the time domain, the frequency domain, or a combination of the two [4]. In a time-domain encoding system, the signal is encoded by time spreading of an optical pulse. The system is spectrally inefficient as a long code word is usually required to maintain a low cross-correlation. In the frequency domain, by using multiple wavelengths for signal encoding, spectral amplitude coding (SAC) OCDM [5] can offer a better spectral efficiency.

Another important advantage of SAC/OCDM is that multiple-access interference (MAI), in theory, can be eliminated by using a balance detection receiver. In addition, unlike other frequency-domain systems that use phase for signal encoding, SAC/OCDM can use incoherent sources, which allows for simpler and cheaper systems. This feature is very important, especially in the access network environment where construction cost is one of the most critical issues.

In this paper, we therefore propose a novel architecture of a LR-PON using SAC/OCDM. To reach a long transmission distance, an Erbium-doped fiber amplifier (EDFA) is located on the link between optical line terminal (OLT) and optical network units (ONUs). Based on proposed architecture, we analyze the effects of EDFA noise, i.e. amplified spontaneous emission (ASE) noise, on the performance of OCDM-based LR-PON. Other noise and interference such as shot noise, thermal noise, beat noise, and multiple-access interference (MAI) are also included in our theoretical analysis and simulation. In order to achieve a good performance, we will try to find the best location to put the EDFA in the network.

The rest of this paper is organized as follows. In Section II, we present the architecture of an OCDM-based LR-PON. The theoretical analysis of the performance of LR-PON is presented in Section III. In Section IV, we show the simulation setup of a OCDM-based LR-PON, the simulation results, and discussion. Finally, Section V concludes the paper.

II. OCDM-BASED LR-PON ARCHITECTURE

A SAC/OCDM-based LR-PON architecture is illustrated in Fig. 1. It consists of a shared fiber that originates from an OLT. At a point close to the customer premises, a passive optical splitter is used to connect each ONU to the main fiber.

At the OLT, downstream traffics sending to K users are encoded by spectral encoders, which can be implemented using the well-studied fiber Bragg grating (FBG) structure [6]. The spectral encoders are controlled by different codes denoted as C_m with $m = 1, 2, \dots, K$. At each spectral encoder, a broadband (multi-wavelength) source, whose number of wavelengths are N_w , is first on-off keying (OOK) modulated

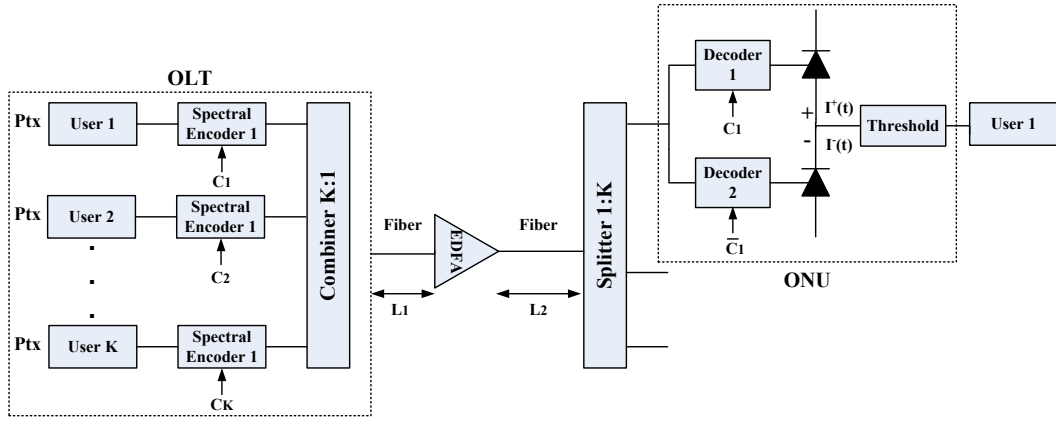


Fig. 1. Block diagram of a SAC/OCDM-based LR-PON.

by binary data. Next, depending on the signature code (C_m), wavelengths corresponding to chips “1” in a signature code are blocked while others can pass through. As a result, each binary bit “1” is represented by a multi-wavelength pulse while no signal is transmitted in case of binary bit “0”. Multi-wavelength pulse from each encoder is then combined at a $K : 1$ combiner and then transmitted into the optical fiber.

To compensate fiber loss and the various coupler losses, an EDFA optical amplifier is placed on the link at the distance of L_1 (km) from OLT while the distance from the EDFA amplifier to the splitter is L_2 (km). All wavelengths are amplified simultaneously while passing through the amplifier thanks to its large bandwidth. The average gain of optical amplifier is denoted as G .

Each ONU receives the signals not only from desired encoder (i.e., data signal) but also from remaining encoders (i.e., MAI signal). There are two decoders at each ONU. The first decoder has the same characteristic with the desired encoder while the second one has reverse characteristic. It means that all wavelengths corresponding to chips “0” of C_m are blocked by the second decoder.

The signature codes used in SAC/OCDM systems are designed to have a fixed in-phase cross-correlation value so that the number of wavelengths passing through each decoder, in the case of an interfering signal (from undesired decoders), are the same. Because the decoded signal from the two decoders is detected by two photodetectors (PD1 and PD2) connected in a balanced fashion on the additive and subtractive branches, all interfering signals (i.e., MAI) can be eliminated [5].

III. THEORETICAL ANALYSIS

In this system, we use the Hadamard code, whose weight and in-phase cross correlation can be represented by its length (N). Let C_m and C_n be two code vectors, the correlation between these two vectors can be expressed as

$$R_{C_m C_n} = \sum_{i=1}^N C_{m,i} C_{n,i} = \begin{cases} N/2 & \text{if } m = n, \\ N/4 & \text{if } m \neq n. \end{cases} \quad (1)$$

Let \mathfrak{R} refers to the responsivity of the photodiode and P_{tx} to transmitted optical power, the data current generated by the optical data signal at the output of PD1 and PD2 can be respectively expressed as

$$\begin{aligned} I_{data}^+ &= \frac{1}{2} \mathfrak{R} G \frac{P_{tx}}{N_w} \left(N_w - \frac{N}{2} \right) 10^{-\alpha(L_1+L_2)/10} \\ I_{data}^- &= \frac{1}{2} \mathfrak{R} G \frac{P_{tx}}{N_w} (N_w - N) 10^{-\alpha(L_1+L_2)/10}, \end{aligned} \quad (2)$$

where α is the fiber attenuation coefficient in dB/km. The total data current, therefore, can be expressed as

$$I_{data} = I_{data}^+ - I_{data}^- = \begin{cases} \frac{1}{2} \mathfrak{R} \frac{P_{tx}}{N_w} \frac{N}{2} 10^{-\alpha(L_1+L_2)/10} & \text{bit 1,} \\ 0 & \text{bit 0.} \end{cases} \quad (3)$$

The photocurrents caused by the MAI signals from interfering encoders when they pass the PD1 and PD2 are given by

$$I_{MAI}^+ = I_{MAI}^- = \frac{1}{2} \mathfrak{R} G \frac{P_{tx}}{N_w} (N_w - N) 10^{-\alpha(L_1+L_2)/10}. \quad (4)$$

Due to ASE that is caused by the amplifier, there is also ASE noise current at the output of two photodetectors, which can be expressed as

$$I_{ASE} = \mathfrak{R} h f n_{sp} (G - 1) B_{opt} 10^{-\alpha L_2/10}, \quad (5)$$

where h is Planck’s constant; f is the optical frequency; B_{opt} is the optical bandwidth; and n_{sp} is the spontaneous-emission factor (or the population-inversion factor).

Other noise that should be taken into account at the ONU include the thermal noise, shot noise, and beat noise. First, the variance of the thermal noise can be written as

$$\sigma_{th}^2 = \frac{4K_B T B}{R_L} \quad (6)$$

where, K_b is Boltzman’s constant, T is the receiver temperature, B is the bit rate, and R_L is the load resistance.

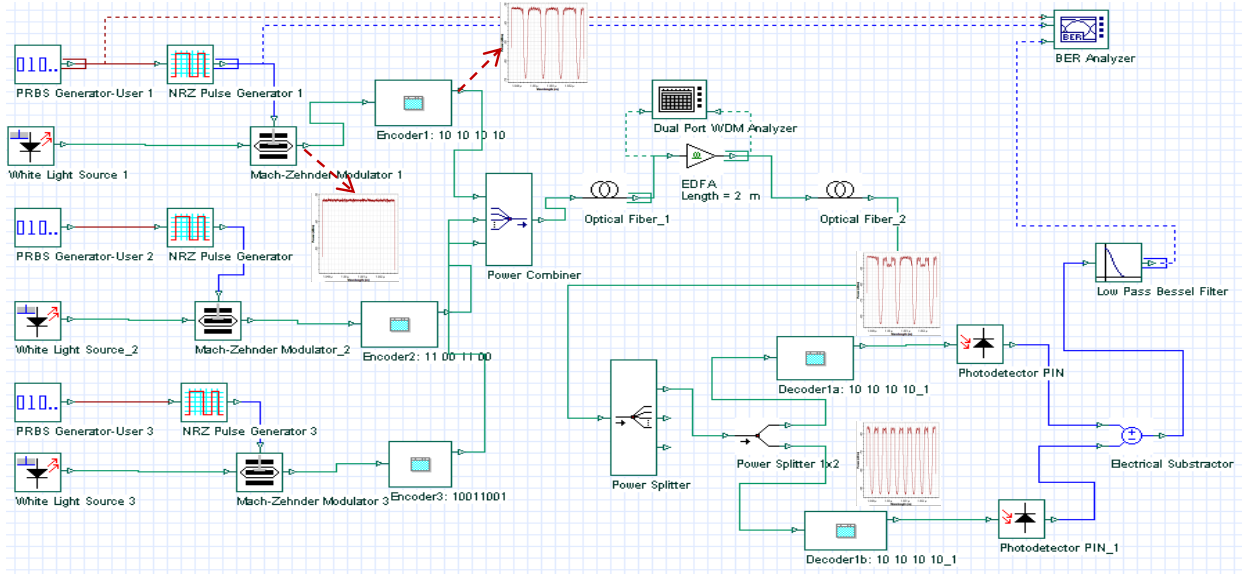


Fig. 2. Simulation model of a SAC/OCDMA-based LR-PON.

$$\begin{aligned}
\sigma_{beat}^2 &= I_{data}^+ I_{ASE} \frac{B}{B_{opt}} + I_{data}^- I_{ASE} \frac{B}{B_{opt}} + \frac{1}{2} \left[\left(\frac{1}{2} I_{ASE} \right)^2 + \left(\frac{1}{2} I_{ASE} \right)^2 \right] \frac{B(2B_{opt} - B)}{B_{opt}^2} \\
&+ 2(K-1) \left(\frac{1}{2} I_{MAI}^+ I_{ASE} + \frac{1}{2} I_{MAI}^- I_{ASE} \right) \frac{B}{B_{opt}} + \frac{1}{2} (K-1) (I_{data}^+ I_{MAI}^+ + I_{data}^- I_{MAI}^-) \frac{B(2B_{opt} - B)}{B_{opt}^2} \\
&+ \frac{1}{2} \left[\frac{K(K-1)}{2} - (K-1) \right] [(I_{MAI}^+)^2 + (I_{MAI}^-)^2] \frac{B(2B_{opt} - B)}{B_{opt}^2} \\
&= \frac{1}{2} \Re^2 B f n_{sp} G (G-1) \frac{P_{tx}}{N_w} \left(2N_w - \frac{3N}{2} \right) 10^{-\alpha(L_1+2L_2)/10} + \frac{1}{4} \Re^2 h^2 f^2 n_{sp}^2 (G-1)^2 B (2B_{opt} - B) 10^{-2\alpha L_2/10} \\
&+ (K-1) \Re^2 B h f n_{sp} G (G-1) \frac{P_{tx}}{N_w} (N_w - N) 10^{-\alpha(L_1+2L_2)/10} \\
&+ \frac{1}{8} (K-1) \Re^2 G^2 \frac{P_{tx}^2}{N_w^2} (N_w - N) \left(2N_w - \frac{3N}{2} \right) \frac{B(2B_{opt} - B)}{B_{opt}^2} 10^{-2\alpha(L_1+L_2)/10} \\
&+ \frac{1}{4} (K-1) \left(\frac{K}{2} - 1 \right) \Re^2 G^2 \frac{P_{tx}^2}{N_w^2} (N_w - N)^2 \frac{B(2B_{opt} - B)}{B_{opt}^2} 10^{-2\alpha(L_1+L_2)/10} \quad (8)
\end{aligned}$$

Next, the variance of the shot noise, which is generated by data, ASE, and MAI signal, is given by

$$\begin{aligned}
\sigma_{shot}^2 &= 2qB (I_{data}^+ + I_{data}^-) + 2qB (I_{MAI}^+ + I_{MAI}^-) \\
&+ 2qB I_{ASE} \\
&= qB \Re G \frac{P_{tx}}{N_w} \left(2N_w - \frac{3N}{2} \right) 10^{-\alpha(L_1+L_2)/10} \\
&+ 2qB (K-1) \Re G \frac{P_{tx}}{N_w} (N_w - N) 10^{-\alpha(L_1+L_2)/10} \\
&+ 2qB R h f n_{sp} (G-1) B_{opt} 10^{-\alpha(L_1+L_2)/10}. \quad (7)
\end{aligned}$$

The last one is beat noise current. It consists of the signal-ASE beat noise, the ASE-ASE beat noise (beating between the spectral components of the added amplifier ASE), the MAI-ASE beat noise and the signal-signal beat noise. The variance of the beat noise is given by Eq. (8).

The total variance of the noise current is the sum of all variances of thermal noise, shot noise, beat noise and can be written as

$$\sigma_{total}^2 = \sigma_{th}^2 + \sigma_{shot}^2 + \sigma_{beat}^2. \quad (9)$$

Finally, The bit error rate (BER) can be calculated as

$$\text{BER} = \frac{1}{2} \text{erfc} \left(\frac{Q}{\sqrt{2}} \right) \quad (10)$$

where $\text{erfc}(\cdot)$ is the complementary error function, and Q is written as [7]

$$Q = \frac{I_{data}(1) - I_{data}(0)}{\sqrt{\sigma_{total}^2(1) + \sigma_{total}^2(0)}}, \quad (11)$$

where $I_{data}(1)$ and $I_{data}(0)$ are the data currents that can be derived from Eq. (3) for bit “1” and bit “0”, respectively. Both

TABLE I
PARAMETERS USED FOR SYSTEM SIMULATIONS.

Name	Symbol	Value
Boltzmann's constant	K_B	1.38×10^{-23} W/K/Hz
Electron charge	q	1.6×10^{-19} C
Load resistor	R_L	1000 Ω
Receiver temperature	T	300 K
PD responsivity	\mathfrak{R}	1 A/W
Length of code word	N	8
Number of wavelengths	N_w	17
Number of users	K	3
Bit rate per user	R_b	1 Gbps

$\sigma_{total}^2(1)$ and $\sigma_{total}^2(0)$ are calculated using Eq. (9). However, when $\sigma_{total}^2(0)$ is computed, the value of I_{data}^+ and I_{data}^- should be zero in all related equations.

IV. SIMULATION SETUP AND RESULTS

A. Simulation Setup

The simulation of SAC/OCDM-based LR-PON is carried out on OptiSystem, a comprehensive software design suite that enables users to plan, test, and simulate optical links in the transmission layer of modern optical networks [8]. The block diagram of the simulation model is shown in Fig. 2. The signal spectrums at the outputs of the modulator, encoder and decoders are also illustrated in the figure.

Three downstream traffics are generated by three *PRBS generators*, which generate pseudo random bit sequences. These bit sequences are then used to control *NRZ generators* to generate non-return-to-zero signals. OOK modulation between a NRZ signal and a multi-wavelength signal that is generated by a *white light source* is carried out by using a *Mach-Zender modulator*. Finally, multi-wavelength OOK signals are encoded at *encoders*, which are constructed from FBGs.

A *power combiner* will combine the signals from different encoders then transmit them into the *first optical fiber*. The signals then will be amplified by an *EDFA amplifier* and input into the *second optical fiber*.

In the receiver side, two *power splitters* are used. The first one is responsible to deliver the signals to all ONUs. The second one is located at each ONU to split the received signals into two parts for two *decoders*, which are also constructed from FBGs. Decoded signals are converted into photocurrents by using two *PIN photodetector* that are connected to a *electrical subtractor* to create a balance detector. Finally, BER of the received signal is analyzed by using a *BER analyzer* in combination with a *low pass Bessel filter*.

B. Simulation Results

Simulations have been carried out to study the effects of EDFA noise on the performance of SAC/OCDM-based LR-PON. Key parameters used for this simulation are listed in Table 1.

We can observe spectrum of signals at the outputs of *modulator*, *encoder* and *decoders* as shown in Fig. 2. After going through the encoder, spectrum of signal is removed $N/2$ (i.e.,

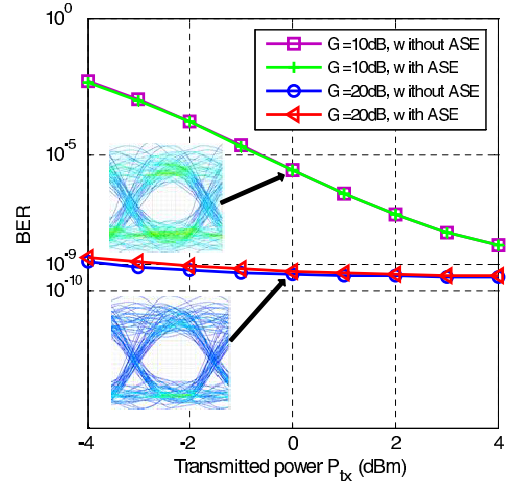


Fig. 3. BER vs. transmitted power (P_{tx}) with $K = 3$ users, $R_b = 1$ Gbps, $L_1 = 30$ km, and $L_2 = 60$ km.

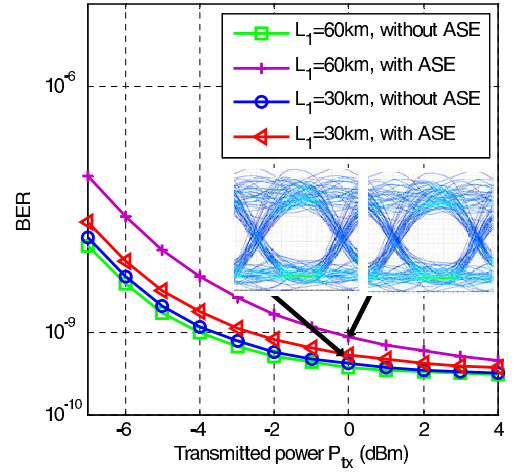


Fig. 4. BER vs. transmitted power (P_{tx}) with $K = 3$ users, $R_b = 1$ Gbps, $G = 20$ dB, and total link distance $L_1 + L_2 = 90$ km.

4) wavelengths. It will be unchanged while passing through decoder 1 and is further removed $N/2$ wavelengths while passing through decoder 2. Thus, the remaining wavelengths in spectrum of the signal at the output of decoder 2 are $(N_w - N)$.

Figure 3 shows how the BER varies with transmitted power for two different values of EDFA gain, i.e., 10 and 20 dB. The EDFA amplifier is fixed at the distance of $L_1 = 30$ km from OLT and $L_2 = 60$ km to ONUs. We evaluate BER for two cases, with and without ASE noise. It is seen that the required transmitted power is reduced when EDFA gain increases from 10 dB to 20 dB. However, when EDFA gain increases, the effect of ASE noise also increases as we can observe in the figure. For the $G = 10$ dB case, two curves with and without ASE are exactly the same because the length of EDFA fiber is short (1 m). Thus, the effect of ASE is inconsiderable.

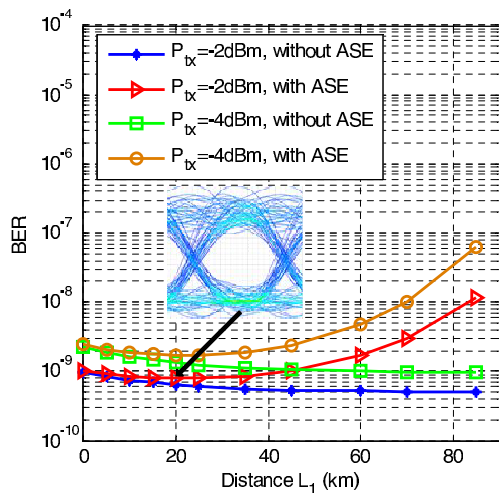


Fig. 5. BER vs. the link distance (L_1) with $K = 3$ users, $R_b = 1$ Gbps, $G = 20$ dB, and total link distance $L_1 + L_2 = 90$ km.

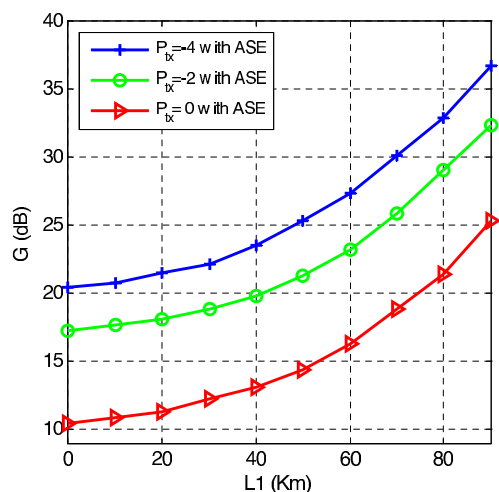


Fig. 6. G vs. the link distance (L_1) with $K = 3$ users, $R_b = 1$ Gbps, $BER = 10^{-9}$ dB, and total link distance $L_1 + L_2 = 90$ km.

In Fig. 4, we fix $G = 20$ dB and total link distance (i.e., $L_1 + L_2$) of 90 km. We investigate BER versus transmitted power for two values of L_1 , $L_1 = 30$ km and $L_1 = 60$ km. We can see that the effect of ASE increases with distance L_1 . More specifically, the power penalty due to ASE noise at BER of 10^{-9} is only 1.5 dB when $L_1 = 30$ km. When $L_1 = 60$ km, it increases to 4 dB. It is because, according to Eq. (5), ASE noise current is inversely proportional to L_2 . It means that I_{ASE} strong when L_2 is short or L_1 is large.

Figure 5 shows the dependence of BER on the position of EDFA amplifier on link for two different values of transmitted

power, $P_{tx} = -4$ dBm and $P_{tx} = -2$ dBm. We can see that, in the absence of ASE, BER reduces when L_1 increases. However, when ASE noise is considered, the longer L_1 is, the worse BER is. The values of L_1 at which the lowest BER can be achieved is the range of 15 km to 25 km.

Other useful information for network design can be obtained from Fig. 6, where the required EDFA gain that is corresponding to a specific distance of L_1 at $BER = 10^{-9}$ can be found. Based on this result, we are able to determine the required EDFA gain corresponding to the specific value of L_1 or the location of EDFA on the link.

V. CONCLUSION

In this paper, we have proposed a model of LR-PON using multi-wavelength OCDM and EDFA. Moreover, we analyzed the effects of EDFA noise on the performance of OCDM-based LR-PON. Other noise and interference such as shot noise, thermal noise, beat noise, and MAI are included in our theoretical analysis and simulation. We found that the location of EDFA on the link between OLT and ONUs plays an important role in network design since it affects on the network performance. According to the numerical results, to achieve low bit error rate, the EDFA should be located around 15 to 25 km from OLT when total link distance (i.e., $L_1 + L_2$) of 90 km.

ACKNOWLEDGMENT

This work has been supported in part by Vietnam National University (VNU-Hanoi) under the project of Teaching Research Improvement Grant (TRIG), The National Foundation for Science and Technology Development (NAFOSTED) and the Project CN.11.08 of University of Engineering and Technology.

REFERENCES

- [1] R. P. Davey, D. B. Grossman, M. Rasztoivts-Wiech, D. B. Payne, D. Nessel, A. R. A. E. Kelly, S. Appathurai, and S.-H. Yang, "Long-reach passive optical networks," *J. of Lightwave Technol.*, vol. 27, no. 3, pp. 273–291, Feb. 2009.
- [2] Shea, D.P.; Mitchell, J.E., "Long-Reach Optical Access Technologies," *IEEE Network*, vol. 21, no. 5, pp. 5–11, Sept.–Oct. 2007.
- [3] A. Stok and E. H. Sargent, "The role of optical CDMA in access networks," *IEEE Commun. Mag.*, vol. 40, no. 9, pp. 83–87, Sep. 2002.
- [4] K. Foully and M. Maier, "OCDMA and optical coding: principles, applications, and challenges," *IEEE Commun. Mag.*, vol. 45, no. 8, pp. 27–34, Aug. 2007.
- [5] D. Zaccarin and M. Kavehrad, "An optical CDMA system based on spectral encoding of LED," *IEEE Photon. Technol. Lett.*, vol. 4, no. 4, pp. 479–482, Apr. 1993.
- [6] A. Grunnet-Jepsen, A. E. Johnson, E. S. Maniloff, T. W. Mossberg, M. J. Munroe, and J. N. Sweetser, "Fiber Bragg grating based spectral encoder/decoder for lightwave CDMA," *Electron. Lett.*, vol. 35, no. 13, pp. 1096–1097, June 1999.
- [7] G. P. Agrawal, *Fiber-Optic Communication Systems*, 3rd edition, A John Wiley & Sons, Inc., Publication, 2002.
- [8] http://www.optiwave.com/products/system_overview.html